Available online at www.sciencedirect.com
ScienceDirect
Journal of Microbiological Methods 71 (2007) 202–211
Journal of Microbiological Methods
www.elsevier.com/locate/jmicmeth

Robotized incubation system for monitoring gases (O_2, NO, N_2O N_2) in denitrifying cultures

Lars Molstad, Peter Dörsch, Lars R. Bakken *

Department of Plant and Environmental Sciences, Norwegian University of Life Sciences, PO box 5003, N-1432 Aas, Norway

Received 22 June 2007; received in revised form 25 August 2007; accepted 29 August 2007
Available online 4 September 2007

Abstract

As genomic data for bacteria are unraveled at an increasing speed, there is a need for more efficient and refined techniques to characterize metabolic traits. The regulatory apparatus for denitrification, for instance, has been explored extensively for type strains, but we lack refined observations of how these and wild type denitrifiers respond metabolically to changing environmental conditions. There is a need for new "phenomic" approaches, and the present paper describes one; an automated incubation system for the study of gas kinetics in 15 parallel bacterial cultures. An autosampler with a peristaltic pump takes samples from the headspace, and replaces the sampled gas with He by reversing the pump. The sample flows through the injector of a micro GC (for determination of N_2, O_2, CH_4, CO_2, N_2O) to the inlet of a chemoluminescence NO analyzer. The linear range for NO is 0.5–10^4 ppmv (CV=2%, detection limit 0.2 ppmv). The gas leakage of N_2 into the system is low and reproducible, allowing the quantification of N_2 production (in flasks with $He+O_2$ atmosphere) with a detection limit of 150–200 nmol N_2 for a single time increment. The gas loss by each sampling is taken into account, securing mass balance for all gases, thus allowing accurate estimation of electron flows to the various terminal acceptors (O_2, NO_2^-, NO, N_2O) throughout the culture's depletion of O_2 and NO_x. We present some experimental results with *Agrobacterium tumefaciens*, *Paracoccus denitrificans* and denitrifying communities, demonstrating the system's potential for unraveling contrasting patterns of denitrification gene expression as a function of concentrations of O_2 and NO in the medium.

Keywords: Denitrification; Genome; Phenomic approaches; Robotization

1. Introduction

As an increasing number of bacterial genes and whole genomes are being sequenced, the searchable databases for functional and regulatory genes are growing and providing an ever richer basis for data mining. This has fostered an increasing interest in systems biology, i.e. the development of mathematical models to predict phenotypic traits from genomic data. However, phenotypic data are scant, and not organized in databases (with a notable exception for yeasts, Fernandez-Ricaud et al., 2006), but buried in free text (publications). Rich phenotype/metabolic datasets are recognized as a key element in systems biology approaches (Kester et al., 1994; Dudley et al., 2005; Van Dien and Schilling, 2006). There is a striking imbalance between the current advances in genomic information, and the scant amount of phenotype data available.

Denitrification is a good example of the imbalance between genomic and phenomic information. Many functional genes and elements of regulatory networks have been revealed for several type strains (Baker et al., 1998; Butler and Richardson, 2005; Rodionov et al., 2005; Zumft and Kroneck, 2007), allowing extensive data mining in whole genome databases for identification of regulons and various interconnections between different regulatory systems for N-oxide transformations (Rodionov et al., 2005). Such genome studies need experimental verification, however; there is a need for more refined comparative physiological experiments on denitrifier gene expression.

In the present paper, we describe a robotized method, which is primarily designed for characterizing denitrifying bacteria (or microbial communities) regarding their gas production/reduction (O_2, NO, N_2O and N_2), hence electron flows to the different

* Corresponding author. Tel.: +47 64965530.
E-mail address: lars.bakken@umb.no (L.R. Bakken).

0167-7012/$ - see front matter © 2007 Elsevier B.V. All rights reserved.
doi:10.1016/j.mimet.2007.08.011

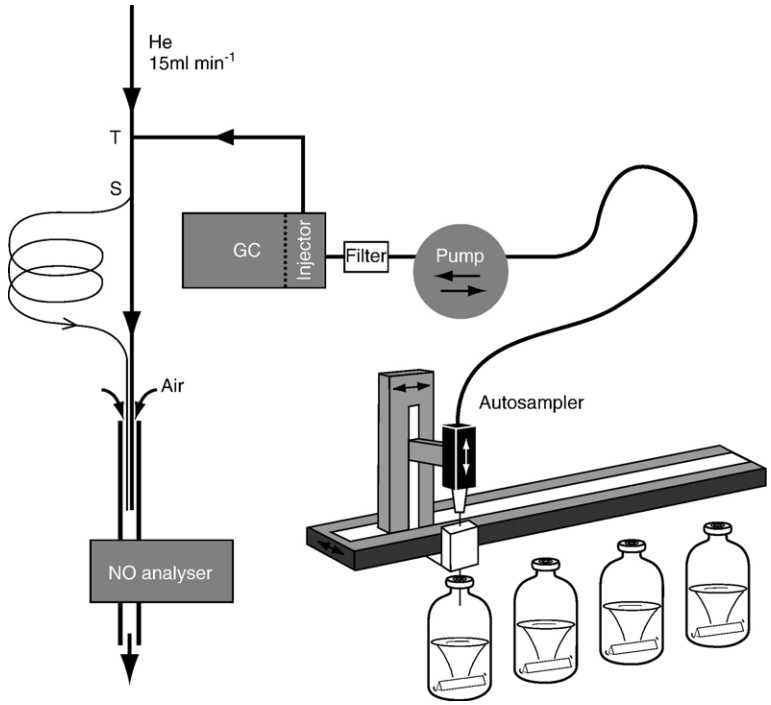

Fig. 1. The sampling and gas analysis system. See text for explanation.

electron acceptors, during and after the transition from oxic to anoxic conditions. Special emphasis has been put on testing the system's ability to monitor the production of N_2 with reasonable precision, thus circumventing the need for using ^{15}N tracer methods or acetylene inhibition of N_2O reductase. Furthermore, we have developed a sensitive and reliable method to monitor NO and O_2, which are both master variables for the regulation of denitrification. Diffusion constraints are taken into account, so as to enable a correct estimation of O_2 concentration in the liquid, based on measured O_2 transport from headspace to the liquid phase.

We believe that the data provided by the system will be valuable counterpoints to the increasing amount of information on regulatory networks in denitrifying bacteria. The system provides rich datasets for denitrification under varying conditions. Ultimately, such data can be used to explore the relationship between genotypes and phenotypes of denitrifying bacteria. Our system's ability to monitor NO in combination with other metabolites adds greatly to its value for the study of denitrification as well as other bacterial NO transformations. NO is recognized as a crucial signal molecule (Poole, 2005; Zumft, 2005), an antimicrobial agent produced by macrophages (Spiro, 2007), and possibly an agent in interactions between bacteria (Choi et al., 2006).

The system can also be used to characterize the ability of bacterial communities to express nitrous oxide reductase (nos) during and after the transition from oxic to anoxic conditions, which appears to have major implications for soil emission of N_2O (Holtan-Hartwig et al., 2002).

The system is described in tedious detail, including various tests of gas leakage and detection capacity. As examples of the system's potentials, we present preliminary data on the kinetics of O_2, NO, N_2O and N_2 production in two type strains, *Paracoccus denitrificans* and *Agrobacterium tumefaciens*, and in a suspension of bacteria extracted from soil by dispersion — density gradient centrifugation.

2. Materials and methods

2.1. Instumentation overview

The incubation system is a thermostated water bath (0–40 °C) with positions for 15 crimp-sealed serum flasks (120 ml) with magnetic stirring, plus 3 positions for standards/blanks without stirring. The stirring device is a 15 position submersible magnetic stirrer (Variomag HP 15, art no 41500 from H+P Labortechnique Gmbh, Munich Germany) controlled by Variomag Telemodul 40 S (H+P Labortechnique GmbH, Munich, Germany). Alternatively, the system can accommodate 28 serum flasks (120 ml) or 129 small serum flasks (12 ml) without stirring.

Headspace gas is sampled periodically by a Gilson Model 222 (Gilson, leBel, France) autosampler and a Gilson Minipuls 3 peristaltic pump (Fig. 1). The needle is a disposable small-diameter steel needle (0.4×40 mm (276×11/2), Braun, Braun-Melsungen Germany), guided through a 1 cm long narrow channel (custom made) to avoid bending. To minimize gas leaks, 1/16" steel tubing is used between pump and needle, and between pump and the GC, except for a small piece of Marprene tubing (id=1 mm od=3 mm, part no 902.0016.016, Watson Marlow, England) in the peristaltic pump. Between the pump and the injection system, there is a filter (External sample filter art no 736729, Varian), which protects the injection system of the GC against particles. The filter restricts the gas flow substantially, thus the gas flow is not identical for up- and

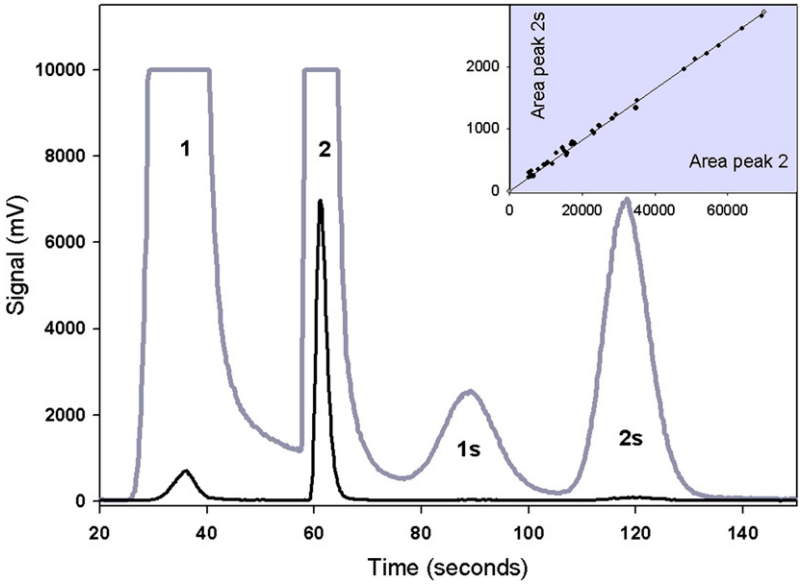

Fig. 2. NO signal peaks from injections of low (black line) and high (grey line) NO concentrations. Peak 1 is the first sample flow which reaches *T* (Fig. 1) during peristaltic pumping, peak 2 is the pulse released by the GC-injector immediately after injection. The peaks 1s and 2s are the delayed peaks from the split loop. Inserted figure shows the close linear relationship between peak 2s and 2, for NO-concentrations ranging from the detection limit for peak 2s to the maximum linear range for peak 2. Regression; (area of peak 2s)=0.041* (area of peak 2), r^2=0.99972.

down-pumping (the restriction reduce mass flow rate by down-pumping, but not the opposite, since flow rate through the peristaltic pump depends on gas pressure on the inlet side but not on the outlet).

The outlet from the sampling loop of the GC is coupled to a T-piece (T, Fig. 1) with He-flow (15 ml min^{-1}) which carries the gas further to the open inlet of a chemoluminiscence NO-analyzer. The inlet of the NO analyser consists of a 60 cm 1/8''

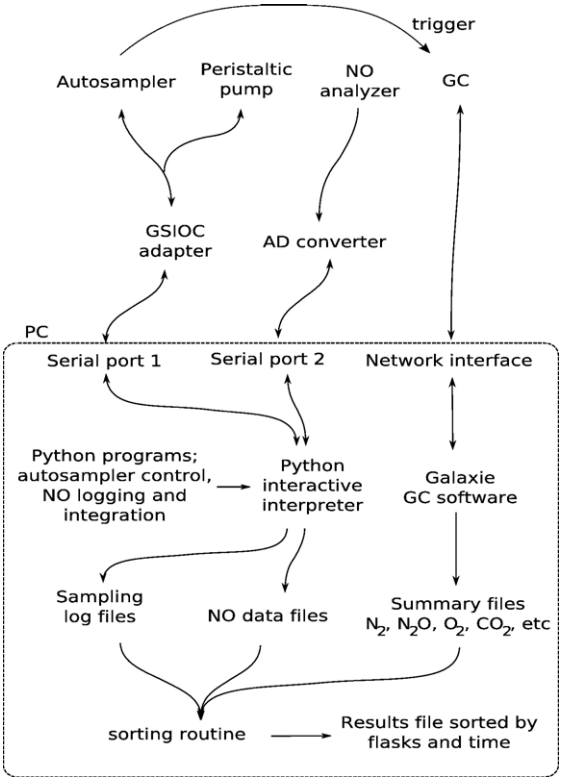

Fig. 3. Overview of instrument controls; signalling, data flows and data filing. See text for explanations.

Table 1
Parameters for gas solubility in water, based on (Wilhelm et al., 1977); see text for explanation

	A cal K^{-1} mol^{-1}	*B* cal mol^{-1}	*C* cal K^{-1} mol^{-1}	*D* cal K^{-2} mol^{-1}	Ostwald coefficient*
O_2	−286.942	15450	36.5593	0.0187662	0.0362
N_2	−327.85	16757.6	42.84	0.0167645	0.0181
CH_4	−365.183	18106.7	49.7554	−0.000285033	0.0405
N_2O	−180.95	13205.8	20.0399	0.0238544	0.785
NO	−333.515	16358.8	45.3253	4.49E-05**	0.0550

Example of calculated gas solubility expressed as L gas per L water at 1 atm partial pressure (Ostwald coefficient) is given in the last column.
*Solubility in L gas L^{-1} water at 1 atm partial pressure, values calculated for 15 °C.
**Estimated by fitting function to reported NO solubilities by the same authors through the temperature range from 273 to 373 K.

tube, which draws air continuously through the instrument (370 ml min^{-1}). The He-line has a split (S, Fig. 1) which diverts 4% of the gas through a split loop (SL) consisting of a 60 cm long 0.5 mm id Peek tube followed by a 120 cm long 1.5 mm id PTFE tube. Both the main He-line (carrying 96% of the sample) and the split loop end approximately 30 cm inside the inlet tube of the NO-analyzer. The He-flow rate by the T-piece is 15 ml/min, which greatly exceeds the flow rate of the sampling pump, thus hindering air from entering the incubation vials when reversing the pump (by down-pumping to replace sampled gas).

The design of the sample transfer to the chemoluminiscence NO analyzer represents a simple solution for analysing NO in small gas samples, compared to that proposed by (Kester et al., 1994). The split loop secures a high linear range for the NO detection. Since the fraction (4%) of the sample flowing through the split loop arrives 60 s later than the main pulse, it appears as a separate peak which is broader than the main peak (peak 2 s versus peak 2, Fig. 2). The side loop thus increases the linear range with a factor of 100 (not 25, since the peak is broader than the main pulse peak). Two typical NO response curves are shown in Fig. 2, one with NO concentrations exceeding the linear range for the main pulse. The absolute detection limit for NO with our injection system is 0.2 ppm (=3 times coefficient of variation for injections from He filled blanks). Linear response was achieved from 0.5 ppmv.

The autosampler and the peristaltic pump are controlled by the computer. The injection program secures that the needle pierces the septa at different places each time, thus minimizing the risk of mechanical leaks. The program also controls the direction, speed and timing of the pumping. By carefully measuring flow rate for up- and down pumping (which will not be equal due to restriction by the gas filter), one can secure that sampled gas is replaced by an equal volume of He. The timing of the pumping can be set so as to ensure that the returned gas volume slightly exceeds the sampled volume (as measured with 1 atmosphere pressure at the needle tip). This results in a build up of a slight overpressure in the incubation flasks (reaching a stable level after a few samplings because the gas flow rate during pumping up from the flask will increase with increasing gas pressure in the flask).

2.2. Analytical instruments

The GC is a Varian CP4900 microGC equipped with two columns (10 m poraPLOT U and 20 m 5 Å Molsieve), with separate injectors and TCD detectors. The GC's own sampling pumps are uncoupled (the system uses the external peristaltic pump), and the system is operated with open injectors (i.e. the sample flow through the two injectors is controlled by the peristaltic pump): The injection time on both columns are 50 ms, column pressure (He) and temperature are 200 kPa and 36 °C for the PLOT U column, and 250 kPa and 50 °C for the Molsieve column.

The NO analyser is a Chemoluminiscence NOx analyser Model 200A (Advanced Pollution Instrumentation, San Diego, USA), measuring NO at high frequency, (20 Hz; NO_2-option disabled, thus NO-signal is recorded continuously). The NO signal is digitalized and the peaks are integrated by a Python

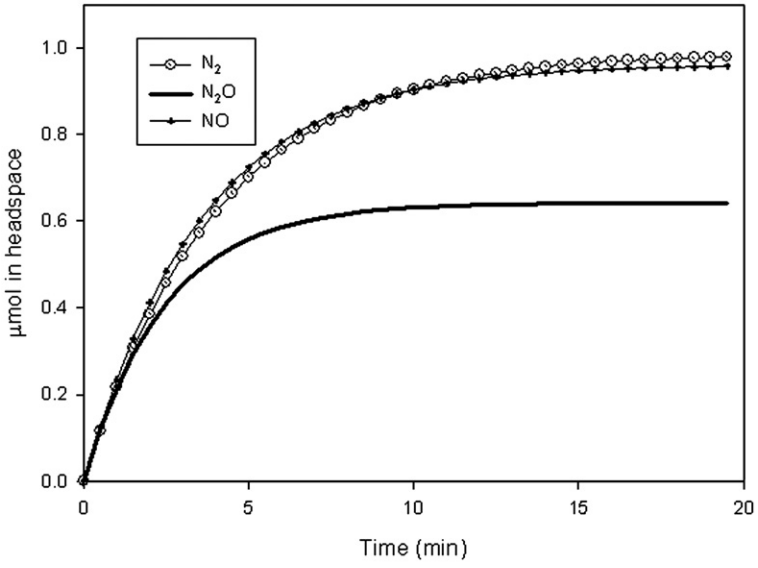

Fig. 4. Calculated gas transport from liquid to headspace for a pulse of 1 mol of N_2, N_2O and NO (temperature 15 °C, volume of water 50 ml, total volume 120 ml).

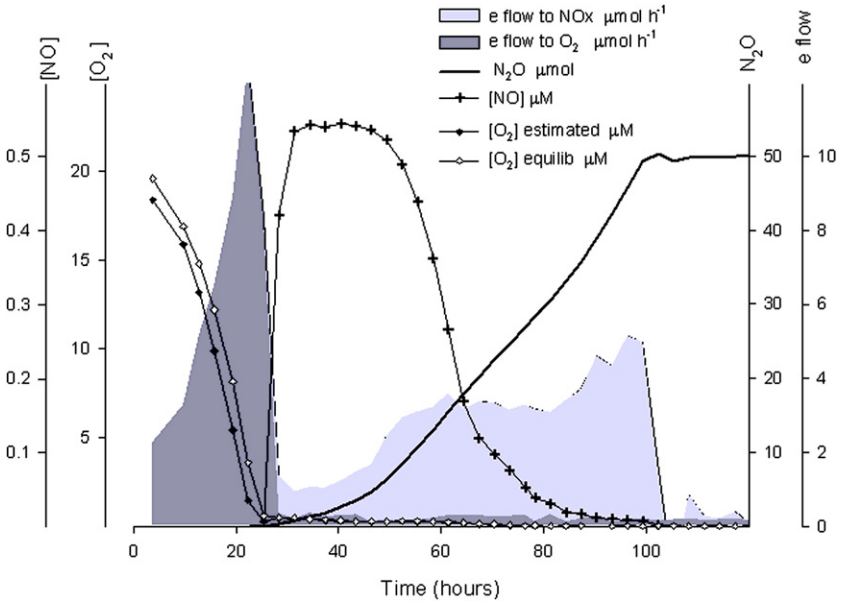

Fig. 5. Gas kinetics and electron flows in *Agrobacterium tumefaciens* during transition from oxic to anoxic conditions. Cells grown in 50 ml Sistrom's medium with 1 mM KNO_3 at 15 °C and initially 1.4 vol% O_2 in headspace. Two O_2 concentrations in the liquid are shown; the estimated concentration as calculated from observed transport rate ([O_2] estimated), and the concentration if in equilibrium with each measurement of O_2 in headspace([O2] equilib). [NO] is the NO concentrations in the liquid (µM), N_2O is µmol N_2O $flask^{-1}$ (losses by sampling are added). Electron flow to O_2 and to NO_x, in µmol $flask^{-1}$ h^{-1} are shown as shaded areas. The data stem from a larger series of incubations by L Bergaust et al., Norwegian University of Life Sciences (manuscript in preparation).

program. Calibration is routinely done by injecting known standards (25 ppm NO in N_2). The present split system secures a linear response over the range 0.5–10^4 ppmv, and the detection limit is approximately 0.25 ppmv (much higher than the detection limit for the instrument, due to dilution).

2.3. Connections, system control and datalogging

Fig. 3 shows an overview of the connections, signalling and data filing of the system. The computer is connected to the autosampler through one of the PC's serial ports (RS232, using a GSIOC cable and adapter from Gilson). The connection with the micro-GC is through a network interface. There is also a cable going from the relay output of the autosampler to an input channel of the GC (trigger, Fig. 3). This cable is used for trigging the GC injector. Another serial port of the PC is used for reading the AD converter connected to the analogue output of the NO analyzer (reading frequency 5 Hz).

The program controlling the autosampler and reading the AD converter is written in the Python programming language, and is normally run from the interactive Python shell. This enables easy debugging and testing (all functions for controlling the pump and autosampler are available at the command prompt).

When a sample is taken, the Python program directs the autosampler and pump to take a sample from a given flask position, and then to trigger the GC injector. The logging of the AD converter from the NO analyzer starts just before the pump starts pumping gas from the flask, and runs in a separate thread in Python. The separate thread is used to allow for the logging to run while the sampling procedure continues.

For each sample taken, the Python program writes a line of text to a log file (the sampling log file). The line of text consists of the time of sampling (trigging time) and an identifier of the flask sampled (i.e. flask position in the rack). The GC data acquisition software (Galaxie, http://www.varianinc.com) provides summary files for all gas peaks except NO-peaks, which are stored by the Python program in separate files (one for each sample). The time of sampling can be found both in the output files of Galaxie and in the NO data files, as well as in the sampling log file written by the Python program. These files are used by a sorting routine which links each chromatogram to a flask and sorts the measurements before presenting them in a spreadsheet.

The control of the pump and the autosampler allows the system to minimize leaks of N_2 and O_2 into the flasks by the sampling, firstly by pumping down (i.e. He-flow through the system, see Fig. 1) continuously between each sampling, secondly by never piercing the septum in the same place twice (using a Halton sequence for piercing within a predefined circle of the septum).

2.4. He washing

A prerequisite for measuring N_2 production is to secure initial low concentrations of N_2. This is done by repeated cycles of evacuation and He-filling. A He-line and a vacuum line are connected via computer-controlled valves to a manifold with 15 flexible steel tubes with Luer fitting for needles at the end. Sterility is secured by mounting 0.2 µm pore size filters between the steel tube and the needle. The needles pierce the septa of the flasks, which are then repeatedly evacuated and filled with He while stirred vigorously (180 s evacuation, 30 s filling with He to 1.5 atm, 6 repeated cycles). The overpressure of He is

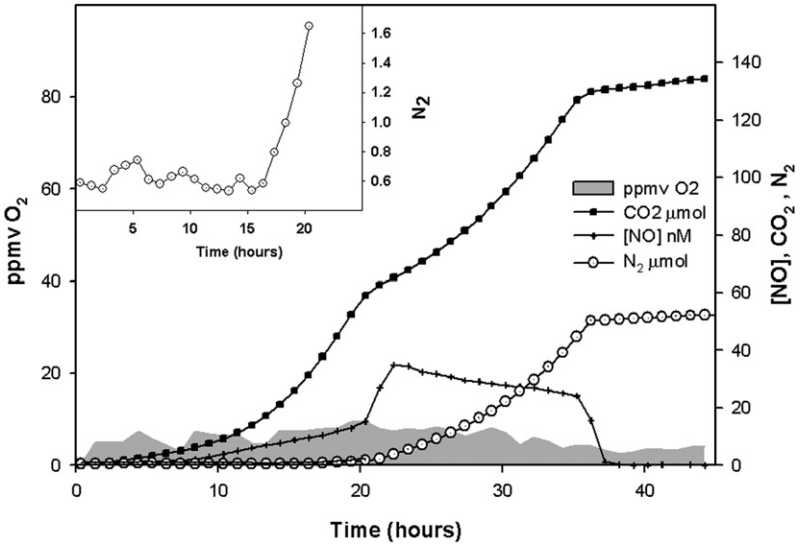

Fig. 6. Incubation experiment with Paracoccus denitrificans grown in 50 ml Sistroms medium (C source, succinate) with 2 mM KNO_3 at 15 °C and initially near zero O_2 in headspace (He atmosphere). CO_2 and N_2 are shown as µmol flask^{-1}. The NO concentrations in the medium [NO] is given as nM. Uncertain estimates of low O_2 concentrations are illustrated by the shaded area (ppmv O_2 in headspace, left axis). Inserted figure shows N_2 (µmol flask^{-1}) during the first 20 h. The data stem from a series of incubations by Bergaust et al., Norwegian University of Life Sciences (manuscript in preparation).

released through a syringe filled with water (no piston) to prevent air entry, and the desired volume of pure O_2 is added by a gastight syringe (and overpressure is released again). He-washing (and subsequent injection of O_2) is routinely done prior to inoculation, to avoid exposure of the inoculum to the anoxic conditions created during He washing.

2.5. Developments and performance testing

Preliminary tests showed that care is needed to avoid gas leaks between the glass and the rubber septa (Brown Crimp seals with rubber septa Cat no 151290, and Macherey-Nagel Rubber stoppers N20 Art no 702-931). A thin film of vacuum grease (Glisseal silicone-free vacuum grease, Borer Chemie AG, Switzerland) and brute force when tightening the crimp seals eliminated such leaks. Gas diffusion through the septa was tested by analysing 7 flasks 24 h after He-washing and then after 40 days storage in air at room temperature.

Each sampling will inevitably result in small inputs of both N_2 and O_2 due to diffusion through the Marprene tubing, the membranes in GC injector, and connections. These inputs were quantified by repeated sampling from flasks filled with He (1 atm.). These gas inputs could be reduced further by enclosing the peristaltic pump in a He-filled chamber (see results), but this was not adopted as a routine.

Other sources of N_2 inputs to the headspace, such as gradual release of N_2 which was not removed by the He-washing (i.e. N_2 remaining in water, the rubber septa and the Teflon cover of the stirring bars), were investigated by monitoring gas concentrations during the first 48 h after He-washing of flasks containing 50 ml sterile water.

Each sampling involves a dilution of the headspace (the sampled gas is replaced with He), which needs to be known to ensure correct mass balance. This dilution was quantified by 25 repeated samplings of 4 flasks (120 ml) initially filled with air. The dilution has also been routinely measured in every subsequent experiment, by including standard flasks with known initial gas concentrations.

When analysing different cultures which produce widely different concentrations of NO or N_2O, the carry over from one culture to the next is a potential problem. We tested this by running a sequence of flasks where every second flask contained pure He, and the others various standard gas mixtures (25 ppmv NO in N_2, 150 ppmv N_2O and 1% CO_2 in He, 21% O_2 in N_2).

The precision of the gas analyses were evaluated by 20 repeated analyses from a series of single flasks. The measured concentrations, corrected for the known dilution by sampling, were used to estimate the coefficient of variation (CV). Since this was expected to be concentration dependent, the experiment was conducted with a series of flasks with widely different initial concentrations of the gases in question (NO, N_2O, N_2, O_2).

The rate of gas transport in/out of the liquid phase is an important characteristic of the system, which needs to be known for a correct calculation of the O_2 concentrations in the liquid. The concentration of dissolved O_2 can be calculated as a function of observed headspace concentrations and transport rates from the headspace to liquid. The transport coefficient cannot be calculated from standard diffusion coefficients since it depends on turbulence and rippling of the liquid surface by the stirring. Hence the transport rate coefficient is system specific (depending on liquid volume per flask, speed of stirring, and temperature), and must be determined experimentally. This was done for a standard condition most frequently used in our lab: 50 ml liquid, 15 °C and maximum stirring speed (=800 rpm). First, 50 ml distilled water was equilibrated to 1 atm pure O_2 in the headspace. This O_2 was then removed by purging the headspace with He (two needles through the septum, rapid He-flow, no evacuation and no stirring during purging), and the O_2 diffusion into the headspace was then monitored during normal stirring until it approached equilibrium.

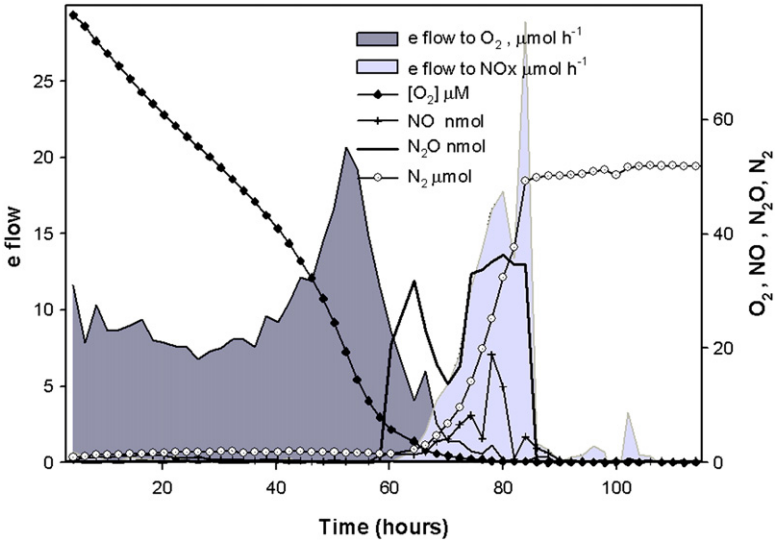

Fig. 7. O_2 depletion and denitrification by suspension of soil bacteria (extracted by dispersion and density gradient centrifugation), incubated in 50 ml mineral salt medium with vitamins, glucose (1 g L^{-1}), HEPES buffer (31 mM, pH = 7), 2 mM NO_3^- and 0.1 mM NO_2^-. The line graphs show the estimated O_2 concentration in the liquid ([O_2] µM), and the amounts of NO (nmol), N_2O (nmol) and N_2 (µmol) in the whole flask (N_2 includes that lost by sampling). The shaded areas shows calculated electron flow to O_2 and NO_x in each time increment. Data stem from a series of incubations by Nicholas Morley et al., Norwegian University of Life Sciences and University of Aberdeen, UK (manuscript in preparation).

Correct estimates of gas production/reduction rates depend on the solubility of each gas. Our calculation of gas solubility for NO, N_2O, N_2 and O_2, are based on Wilhelm et al. (1977), calculating the mole fraction (mol gas per mol water) of each gas as $X_2 = e^{(A + B/T + C^*\ln(T) + D^*T)/R}$, where T is temperature (K), R is 1.9872 cal mol^{-1} K^{-1}; A, B, C, and D are parameters (individual values for each gas) given in Table 1. We identified an error in Wilhelm et al. (1977); the parameter D for NO should be $4.493 * 10^{-5}$ cal K^{-2} mol^{-1}, for the function to comply with NO solubilities reported by the same authors. Equilibrium concentrations of CO_2 and carbonates are calculated as a function of temperature (T, °K) and pH, according to Stumm and Morgan (1996).

Performance of the system is exemplified by selected data from O_2 depletion experiments with *A. tumefaciens* (which lacks N_2O reductase), *P. denitrificans*, and suspensions of soil bacteria extracted from soil by density gradient centrifugation (Aakra et al., 2000).

3. Results

3.1. Gas leaks

The measured leak rate through the septum during the 40 days storage ranged from 13 to 30 nmol N_2 day^{-1} and from 10 to 24 nmol O_2 day^{-1}. The similar leak rates for N_2 and O_2 suggest that the leakage is primarily by diffusion through the septum rubber (not through open channels), since there is normally a 3–4:1 ratio between diffusion coefficient for O_2 versus that of N_2 in polymers (Haraya and Hwang, 1992; Polotskaya et al., 1999). Higher leak rates (and with N_2:O_2 ratios closer to that in the atmosphere) have been encountered when septa were pierced by a partly damaged needle.

The injection system is a more serious source for O_2 and N_2 contamination (carried with the He-flow when pumping down). By pumping He through the system (pumping down) when idle (i.e. between each sampling), the diffusion of N_2 and O_2 into the needle was minimized. Nevertheless, the average contamination by sampling was found to be 61 nmol N_2 (ranging from 53 to 73) and 22 nmol O_2 (range 19–24) per injection. Enclosing the pump in a He-filled chamber lowered the leak to approximately 21 nmol N_2 and 12 nmol O_2 per injection. Such He-enclosure is costly and time consuming to sustain, however, and has not been adopted as a routine. But the experiment helped to identify the peristaltic pump as the main source of N_2 and O_2 leaks into the system. In subsequent incubation experiments, we found the contamination through the injection system is consistently low, but somewhat variable (range 60–120 nmol N_2, 20–50 nmol O_2 per injection), possibly depending on variable leaks in the connections between steel tubing and the rubber tube. As a consequence, control flasks with He are included in every incubation experiment where N_2 production is to be quantified.

Another source of contamination is the release of N_2 and O_2 which remain absorbed in the rubber septa and Teflon cover of the magnetic bar after a standard He wash procedure. Immediately after a He-wash, this emission was 150–200 nmol N_2 and 50 nmol O_2 h^{-1} and gradually declined to reach very low rates after 10–15 h. Standard procedure is thus to He-wash the flasks at least one day before inoculation, to secure a stable background of O_2 and N_2 before inoculation.

3.2. Memory effects, dilution by sampling, and precision

When analysing different cultures which produce widely different concentrations of NO or N_2O, the carry over from one culture to the next is a potential problem. As programmed, however, the injection system is efficiently cleaned between each sampling by the pumping of He through the system during

the entire chromatogram of each sample (180 s). The measured carry over was found to be less than 0.1%.

The sample gas flow during pumping from the flasks is 8.2 ml min^{-1}. It was found necessary to pump for 30 s to ensure that sample gas reached the T-piece (seen as a rising NO signal, Fig. 2), thus 4.2 ml is withdrawn from the flask for each sampling. The gas flow when pumping down (after the injection by the GC) is 10% lower due to the restriction by the filter between the pump and the GC, and the down-pumping was thus prolonged to 33.4 s to maintain 1 atmosphere after sampling. The dilution of the headspace gas by each sampling (as measured by repeated samplings of 120 ml flasks filled with air) was 1.6% throughout the entire sampling series, equivalent to 1.9 ml gas replaced by He for each sampling. Thus, a substantial fraction of the sampled headspace gas was returned to the flask by the down-pumping after GC-injection. Control flasks (no bacteria) are routinely included in experiments to calibrate the GC as well as to assess the dilution. The dilution rate appears to vary somewhat between experiments (but is constant within each), possibly depending on variable tightening of the peristaltic pump.

The precision of the gas analyses as evaluated by 20 repeated analyses from single flasks (corrected for the dilution by sampling), demonstrated a low but concentration-dependent variability. For high concentrations of N_2 and O_2 (10,000 ppmv) and N_2O (150 ppmv), the coefficients of variation (CV) were 0.4–0.5%. For concentrations much below ambient, the CV was somewhat higher: 1.3% for O_2 at 800 ppm, and 0.7% for N_2 at 2500 ppmv. For NO, the standard deviation was approximately 2% (determined for a 25 ppmv NO-standard diluted to 5 ppmv in He). Measurements of very low concentrations of O_2 and N_2 (10–50 ppmv) were more variable, since they are affected by minor but variable air contamination during pumping.

The absolute detection limit for N_2 production during a single time increment (between two samplings) was evaluated based on N_2 data from sterile control flasks. The calculated ΔN_2 for 20 increments, defined as the apparent changes in N_2 for each increment (after correcting for the dilution and leak per injection), had an average close to zero (-2.5 nmol N $flask^{-1}$ $injection^{-1}$) and a standard deviation of 54 nmol N_2 $flask^{-1}$. This would imply that the detection limit for N_2 production in a single increment is 160 nmol N_2 $flask^{-1}$ $injection^{-1}$ (=3 times the standard deviation).

3.3. Diffusion rates between liquid and headspace

In theory, the O_2 transport between the liquid phase and the headspace is a function of the concentrations in the two phases, O_2 solubility, and a coefficient for transport of O_2 between the liquid and the headspace:

Transport between liquid and headspace

$$V = k_{t*}(k_{H*}P_{O2} - [O_2]) \quad (1)$$

Where

- $-V$ is the transport rate (mol O_2 s^{-1})
- $-k_t$ is the coefficient for transport from gas to liquid (L s^{-1})
- $-P_{O_2}$ is O_2 partial pressure in headspace (atm)
- $-k_H$ is the solubility of O_2 in water (mol L^{-1} atm^{-1})
- $-[O_2]$ is O_2 concentration in the liquid (mol L^{-1})

Measured O_2 transport from O_2-saturated distilled water to a He-flushed headspace (see Materials and methods section) was used to estimate k_t. We ran 4 independent experiments at 20 °C, with 50 ml distilled water per flask, measuring O_2 accumulation in the headspace every 210 s over a period of 1050 s after starting the stirring. The model (i.e. Eq. (1) plus the known dilution of the headspace by each sampling) was fitted to the data, and yielded K_t values ranging from 2.7 to $2.8 * 10^{-4}$ L s^{-1}.

Solving Eq. (1) for $[O_2]$ gives $[O_2]=k_H P_{O_2} - V/k_t$, which can be used to calculate average O_2 concentration in the liquid for each time increment between two samplings (estimating V by the difference between measured P_{O_2} in the first sample (corrected for the dilution by the same sampling) and the measured P_{O_2} in the subsequent sample).

The transport coefficient can also be used to evaluate the time it takes to reach equilibrium between liquid and headspace for the other gases produced in the liquid. The transport rate of a gas to the headspace, dn/dt is given by the equation for V above (Eq. (1)). When integrated, Eq. (1) gives

$$n(t) = (n(0) - b/a)e^{-at} + b/a \quad (2)$$

where

$$a = k_t\left(k_H RT/V_g + 1/V_w\right) \quad (3)$$

and

$$b = k_t n_{tot}/V_w. \quad (4)$$

Here, $n(t)$ is the amount of gas in headspace (mol), $n(0)$ is the initial amount of gas in headspace, n_{tot} is the total amount of gas, R is the gas constant (0.082 L atm K^{-1} mol^{-1}), T is temperature (K), V_g is the volume of liquid (L), V_w is the volume of water (L), k_H is the solubility and k_t is the transport coefficient.

We can assume that the transport coefficients (k_t) for the other gases than O_2 can be estimated as $k_t D_g/D_{O_2}$, where D_{O_2} and D_g are diffusion coefficients (in water) for O_2 and the gas in question, respectively, and k_t is the system specific transport coeffieicnt for O_2. The diffusion coefficients at 15 °C are; 1.67, 1.62, 1.67 and 1.52 ($*10^{-5}$ cm^2 s^{-1}) for O_2, N_2O, NO, and N_2, respectively (data from Lide (2005) and Zacharia and Deen (2005); the Wilke-Chang correction (Wilke and Chang, 1955) was used to obtain D for N_2 and NO).

Assume that the bacteria emit a pulse of 1 μmol of NO, N_2O or N_2 in a flask with zero concentration of the gas in headspace, i.e. $n_{tot}=1$ μmol and $n_o=0$. The curves for $n(t)$ for the three gases are shown in Fig. 4.

3.4. Denitrification experiments, mass balances and kinetics

Fig. 5 shows an experiment with *A. tumefaciens* grown in Sistrom's medium (Lueking et al., 1978) containing 1 mM KNO_3. The culture was allowed to deplete O_2 by its own respiration. The estimated O_2 concentrations in the liquid

medium ([O_2] estimated; in this case the plotted values are the average of the two encompassing time increments) are only slightly below the equilibrium concentrations ([O_2] equilib, i.e. the concentration if in equilibrium with measured P_{O_2} in headspace) during the entire oxic phase. NO accumulated to 500 nM in the liquid (220 ppmv in the headspace). The N_2O reached a stable plateau (as NO_3 was depleted, not shown) at 24.7 μmol N_2O = 49.4 μmol N_2O–N per flask (NB; these values include losses by sampling dilution), which is 98.8% of the initial amount of NO_3–N (= 50 μmol per flask). There was no detectable N_2 production (not shown), confirming that *A. tumefaciens* lacks nitrous oxide reductase. Similar recoveries (±5%) of added nitrate – or nitrite – N (as N_2O) have been observed in 50 equivalent incubations with *A. tumefaciens* under varying conditions.

Fig. 5 also illustrates the electron flow rate to O_2 and to NO_x; the latter is based on observed equilibrium NO_2^- concentrations at 20–40 μM (= 1–2 μmol/flask) during the entire period with active denitrification (not shown). The transition from O_2 respiration to denitrification is seen to represent a severe reduction in energy flow for *A. tumefaciens*.

Fig. 6 is an example of the experiments conducted with *P. denitrificans* grown in 50 ml Sistrom's medium (C source, succinate), buffered with 20 mM phosphate, initial pH = 6.5, and initial O_2 concentration near zero. The final N_2 plateau (which includes that lost by sampling) was 52 μmol per flask, which is 104% of the NO_3-N of the medium. The NO concentration plateau during active denitrification is one order of magnitude lower than for *Agrobacterium*. In this particular pH treatment, N_2O was not detected (but was at lower pH levels). The detection limit for N_2O (0.5 ppmv) is equivalent to 2.5 nmol per flask. The CO_2 accumulation appears to slow down after 20 h, coinciding with the sharp increase in NO and N_2 accumulation. This is most probably an artefact, however, caused by the inevitable alkalinisation of the medium by denitrification (the CO_2 accumulation was calculated assuming constant pH = 6.5). This illustrates the limited value of measuring CO_2, unless pH is carefully monitored. The insert in Fig. 6 shows the N_2 data in detail for the first 20 h, which strongly suggest a significant N_2-production starting at least 5 h before the sharp rise in NO. Prior to that (15–17 h), any N_2 production is below the detection limit for the system (which is 150–200 nmol $flask^{-1}$ h^{-1}).

To illustrate the problem with determination of low levels of O_2, we have included the measured concentrations (ppmv in headspace) as a shaded area. The variable but low O_2 concentrations prove that *Paracoccus* is actively respiring O_2 during the entire period of denitrification, consuming practically all the O_2 which leaks into the system due to sampling (19–25 nmol O_2 $flask^{-1}$ $sampling^{-1}$, equivalent to 6–8 ppmv O_2 $sampling^{-1}$).

Fig. 7 shows an example from a series of experiments where bacteria were extracted from soil by dispersion density gradient centrifugation and then incubated under different conditions (Nick Morley et al., unpublished). The experimental conditions are given in the figure legend. As for the other experiments, there is a good (96%) recovery of added $NO_3^- + NO_2^-$ as N_2. The NO levels are comparable to those in *Paracoccus* (1 nmol/flask is equivalent to 0.76 nM in the liquid). Denitrification starts before O_2 is depleted, and is first detected as an increase in NO and N_2O (after 58 h), and then as N_2 (after 64 h). The apparent lag in N_2 accumulation could be taken to suggest that the expression of N_2O reductase lags behind that of NO_2 and NO reductase. This is uncertain, however, since the detection limit for N_2 production is approximately two orders of magnitude higher than that for NO and N_2O (not due to lower instrument sensitivity, but due to variable contamination by atmospheric N_2 in the sampling apparatus, see previous discussion).

4. Discussion

We have described the system in detail to provide a basis for the construction of similar systems by others. For the same reason, we have described a variety of tests, and demonstrated its potentials as well as limitations. Numerous details are important for making a robot of this kind, and to run successful experiments with it. It is far from trivial to measure the kinetics of N_2 production by denitrification without isotopes or inhibitors. Neither is it trivial to measure NO kinetics in bacterial cultures, or to run batch experiments with proper mass balance for gases despite frequent sampling from headspace. We believe, that this kind of instrumentation can generate valuable information for a number of purposes, and foresee the construction of similar robots elsewhere. All the components are commercially available, except for the custom made racks, the needle guide on the autosampler, and the various programs controlling the instruments, signal integration, filing and sorting the data.

The experimental results presented are examples from ongoing studies with denitrification, and demonstrates some of the potentials of the system. The measured coefficient of gas transport between headspace and liquid (Fig. 4) implies that near steady state conditions can be assumed for all gases other than O_2, except during periods with abrupt changes in gas production/consumption. Rapid NO oscillations, as observed by mass spectrometry with direct membrane inlet from cultures of *P. denitrificans* (Kunak et al., 2004; Spiro, 2007), would be impossible to observe, however. The oscillations had a period ranging from approximately 1.5 to 20 min; the latter could possibly be detected (although damped by diffusion), if sampled at maximum frequency (3 min between each sampling). It appears unproblematic to calculate O_2 in the liquid phase from measured O_2 transport from the headspace (Fig. 5). Refinements of the calculation of [O_2] are of course possible, by explicit modelling of respiration and transport.

The determination of N_2 production (and mass balance) is unproblematic, thus circumventing the need for ^{15}N tracer techniques or N_2O reductase inhibition (acetylene). The detection limit for N_2 production is rather high compared to that for NO and N_2O, however (200 nmol $flask^{-1}$ h^{-1}), as illustrated in the insert of Fig. 6.

The frequency of sampling is a bottleneck of the system. Each analysis takes 200 s, thus the frequency of sampling cannot exceed 1 h^{-1} if 15 cultures (plus three unstirred blanks) are run in parallel. When screening different cultures, which may deplete O_2 at different rates, it would be desirable to allow

the frequency of sampling from each flask to be determined by its O_2 level (increasing the frequency as O_2 is being depleted). This is feasible with the present system, but has not yet been programmed. Similarly, it is possible to program the injection system to provide frequent doses of O_2 (or any other gas) to the flasks, thus programming individual concentrations to be sustained over a period of time.

The system is also suited for measuring oxidation of methane, and any other gas which can be quantified by the GC. It may also be used to study the effect of NO on the metabolism of bacteria, which will require monitoring of NO concentrations due to its instability. NO appears to play an important role in microbial interactions, both in the environment and in the gut, as well as being one of the antimicrobial agents of macrophages (Spiro, 2007).

It is possible to quantify Ne with the present setup of the GC, and this can be used as a tracer for dilution (if spiked to much higher levels than its ambient concentration of 18 ppmv). It would also be desirable to mount a pressure sensor behind the sampling needle, to enable the computer to regulate the pressure (via control of the peristaltic pump).

In principle, the 15 cultures could be run as continuous cultures. Continuous culture is often preferred for studies of regulation, since it is better suited for altering one variable at a time (keeping all other conditions constant). However, batch cultures are suitable for a number of experiments with denitrifying bacteria, if designed properly. One obvious prerequisite is that the initial O_2 concentration should be low enough to ensure depletion long before the batch cultures approach their stationary phase (by depleting other resources than O_2).

To our knowledge, there exist no other commercial or custom-made instruments that can match our robot regarding high throughput and richness of the datasets for the kinetics of denitrification. In our lab, the robot has provided uniquely refined data for several denitrifying bacteria under a variety of conditions (manuscripts in preparation). We are also using it for comparative studies of culture collections of denitrifying bacteria regarding their response to oxygen, their consecutive or concomitant expression of the three reductase genes (nir, nor, nos), the NO concentrations sustained during active denitrification, and the reduction of N_2O to N_2. Previous comparative studies of denitrifying communities (Holtan-Hartwig et al., 2002) were done with a more conventional gas chromatographic approach, lacking the ability to monitor O_2 and NO, and required the use of acetylene inhibition of nitrous oxide reductase to assess the production of N_2. The present system opens up for much more refined comparative studies of denitrifying communities, to enhance our understanding of the biological component in regulating the emission of NO and N_2O to the atmosphere.

References

Aakra, A., Hesselsoe, M., Bakken, L.R., 2000. Surface attachment of ammonia-oxidizing bacteria in soil. Microbial Ecology 39, 222–235.

Baker, S.C., Ferguson, S.J., Ludwig, B., Page, M.D., Richter, O.M.H., van Spanning, R.J.M., 1998. Molecular genetics of the genus Paracoccus: metabolically versatile bacteria with bioenergetic flexibility. Microbiology and Molecular Biology Reviews 62, 1046–1078.

Butler, C.S., Richardson, D.J., 2005. The emerging molecular structure of the nitrogen cycle: an introduction to the proceedings of the 10th annual N-cycle meeting. Biochemical Society Transactions 33, 113–118.

Choi, P.S., Naal, Z., Moore, C., Casado-Rivera, E., Abruna, H.D., Helmann, J.D., Shapleigh, J.P., 2006. Assessing the impact of denitrifier-produced nitric oxide on other bacteria. Applied and Environmental Microbiology 72, 2200–2205.

Dudley, A.M., Janse, D.M., Tanay, A., Shamir, R., Church, G.M., 2005. A global view of pleiotropy and phenotypically derived gene function in yeast. Molecular Systems Biology 1–11. doi:10.1038/msb4100004 Article number: 2005.0001.

Fernandez-Ricaud, L., Warringer, J., Ericson, E., Glaab, K., Davidsson, P., Nilsson, F., Kemp, G.J.L., Nerman, O., Blomberg, A., 2006. PROPHESY — a yeast phenome database, update 2006. Nucleic Acid Research 35, D463–D467.

Haraya, K., Hwang, S.T., 1992. Permeation of oxygen, argon and nitrogen through polymer membranes. Journal of Membrane Science 71, 13–27.

Holtan-Hartwig, L., Dorsch, P., Bakken, L.R., 2002. Low temperature control of soil denitrifying communities: kinetics of N_2O production and reduction. Soil Biology & Biochemistry 34, 1797–1806.

Kester, R.A., Wijlhuizen, A.G., Duyts, H., Laanbroek, H.J., 1994. Chemoluminiscence analysis of nitric oxide in small-volume samples by a modified injection method. Biology and Fertility of Soils 18, 260–262.

Kunak, M., Kucera, I., van Spanning, R.J.M., 2004. Nitric oxide oscillations in *Paracoccus denitrificans*: the effects of environmental factors and of segregating nitrite reductase and nitric oxide reductase into separate cells. Archives of Biochemistry and Biophysics 429, 237–243.

Lide, D.R., 2005. Handbook of Chemistry and Physics. CRC Press.

Lueking, D.R., Fraley, R.T., Kaplan, S., 1978. Intracytoplasmic membrane synthesis in synchronous cell populations of Rhodopseudomonas sphaeroides. Fate of "old" and "new" membrane. Journal of Biological Chemistry 253, 451–457.

Polotskaya, G.A., Andreeva, D.V., El'yashevich, G.K., 1999. Investigation of gas diffusion through films of fullerene-containing poly(phenylene oxide). Technical Physics Letters 25, 555–557.

Poole, R.K., 2005. Nitric oxide and nitrosative stress tolerance in bacteria. Biochemical Society Transactions 33, 176–180.

Rodionov, D.A., Dubchak, I.L., Arkin, P.A., Alm, E.A., Gelfand, M.S., 2005. Dissimilatory metabolosm of nitrogen oxides in bacteria: comparative reconstruction of transcriptional networks. PLoS Computational Biology 1, 0415–0431.

Spiro, S., 2007. Regulators of bacterial responses to nitric oxide. Fems Microbiology Reviews 31, 193–211.

Stumm, W., Morgan, J.J., 1996. Aquatic Chemistry. Wiley Interscience. 1–1022 pp.

Van Dien, S., Schilling, C.H., 2006. Bringing metabolomics data into the forefront of systems biology. Molecular Systems Biology 2, 1–2. doi:10.1038/msb4100078 Art. No. 2006.0035.

Wilhelm, E., Battino, R., Wilcock, R.J., 1977. Low-pressure solubility of gases in liquid water. Chemical Reviews 77, 219–262.

Wilke, C.R., Chang, P., 1955. Correlation of diffusion coefficients in dilute solutions. American Institute of Chemical Engeneers Journal 1, 264–270.

Zacharia, I.G., Deen, W.M., 2005. Diffusivity and solubility of nitric oxide in water and saline. Annals of Biomedical Engineering 33, 214–222.

Zumft, W.G., 2005. Nitric oxide reductases of prokaryotes with emphasis on the respiratory, heme-copper oxidase type. Journal of Inorganic Biochemistry 99, 194–215.

Zumft, W.G., Kroneck, P.M.H., 2007. Respiratory transformation of nitrous oxide (N_2O) to dinitrogen by Bacteria and Archaea. Advances in Microbial Physiology vol 52, 107–227.